Cell. Mol. Life Sci. 64 (2007) 2702 – 2715
1420-682X/07/192702-14
DOI 10.1007/s00018-007-7316-3

Cellular and Molecular Life Sciences

Research Article

CAP2, cyclase-associated protein 2, is a dual compartment protein

V. Peche[a, †], S. Shekar[a, †], M. Leichter[a, †, +], H. Korte[a], R. Schröder[c], M. Schleicher[d], T. A. Holak[e], C. S. Clemen[a], B. Ramanath-Y.[f], G. Pfitzer[b, f], I. Karakesisoglou[a] and A. A. Noegel[a, b, *]

[a] Institute of Biochemistry I, Medical Faculty, University of Cologne, Joseph-Stelzmann-Str. 52, 50931 Köln (Germany), Fax: +49-221-478-6979, e-mail: noegel@uni-koeln.de
[b] Center for Molecular Medicine Cologne, Medical Faculty, University of Cologne, 50931 Köln (Germany)
[c] Institute of Neuropathology, Friedrich-Alexander University Erlangen-Nürnberg, Medical Faculty, 91054 Erlangen (Germany)
[d] Institute of Cell Biology, Ludwig-Maximilians University, 80336 München (Germany)
[e] Max-Planck-Institute of Biochemistry, 82152 Martinsried (Germany)
[f] Institute of Vegetative Physiology, Medical Faculty, University of Cologne, 50931 Köln (Germany)

Received 12 July 2007; received after revision 14 August 2007; accepted 22 August 2007
Online First 6 September 2007

Abstract. Cyclase-associated proteins (CAPs) are evolutionarily conserved proteins with roles in regulating the actin cytoskeleton and in signal transduction. Mammals have two CAP genes encoding the related CAP1 and CAP2. We studied the distribution and subcellular localization of CAP1 and CAP2 using specific antibodies. CAP1 shows a broad tissue distribution, whereas CAP2 is significantly expressed only in brain, heart and skeletal muscle, and skin. CAP2 is found in the nucleus in undifferentiated myoblasts and at the M-line of differentiated myotubes. In PAM212, a mouse keratinocyte cell line, CAP2 is enriched in the nucleus, and sparse in the cytosol. By contrast, CAP1 localizes to the cytoplasm in PAM212 cells. In human skin, CAP2 is present in all living layers of the epidermis localizing to the nuclei and the cell periphery. In *in vitro* studies, a C-terminal fragment of CAP2 interacts with actin, indicating that CAP2 has the capacity to bind to actin.

Keywords. CAP/Srv2, CAP1, actin cytoskeleton, nuclear actin binding protein, myofibrils, M-line, skin, tumor array.

Introduction

The actin cytoskeleton participates in many fundamental cellular aspects including the regulation of cell shape, motility, and adhesion. Its remodeling depends on actin binding proteins, which organize actin filaments into specific structures that allow the participation in various specialized functions [1]. One family of proteins essential for maintaining the equilibrium between G- and F-actin is the monomer actin binding protein or G-actin sequestering protein family. CAP (cyclase-associated protein) belongs to this family and its homologs in yeast, *Dictyostelium*

† These authors made an equal contribution to this work.
+ Present address: RNA Processing Lab, Institute of Biological Research and Biotechnology, The National Hellenic Research Foundation, 48 Vas. Constantinou Ave., 11635 Athens (Greece).
* Corresponding author.

and mammals have been shown to sequester G-actin through their C-terminal domain [2, 3].

CAP is a highly conserved and widely distributed protein. It was first described in yeast, where it was independently identified as an adenylyl cyclase-associated protein by genetic and biochemical methods. In addition to its requirement for the activation of adenylyl cyclase, it is also essential for normal actin organization by binding to G-actin and regulating actin filament dynamics. CAP has been found in plants, yeast, *Dictyostelium*, *Drosophila* and mammals. Loss of CAP results in defects in cell morphology, migration, endocytosis and development [4, 5]. CAPs are multifunctional proteins with a tripartite modular structure. The N-terminal domain of the *Saccharomyces cerevisiae* CAP/Srv2 binds to adenylyl cyclase and serves as an effector of Ras during nutritional signaling, the N-domains of CAPs from other organisms do not appear to interact with adenylyl cyclases [4]. The N-domain of the *Dictyostelium* protein functions in dimerization, mediates the cortical localization of the protein and supports its functions in cell polarity and development [6, 7]. The N-domain is separated from the C-domain by a proline-rich sequence. This sequence allows binding to multiple SH3 domain-containing proteins such as ABP1 in yeast, a F-actin binding protein that is responsible for the cytoskeletal localization of yeast CAP/Srv2 [8]. The C-terminal domain binds to G-actin and mediates oligomerization [9].

The structures of the N- and the C-domain of CAP have been solved recently [10–12]. An N-terminal fragment of *Dictyostelium* CAP comprising residues 51–226 is an α-helix bundle composed of six antiparallel helices. The crystal structure of the C-terminal dimerization and G-actin binding domain of the yeast protein revealed an unusual dimer with each monomer comprised of β-sheets and connecting loops arranged into a helix. The dimer is formed by the exchange of the last two strands of each monomer.

Higher eukaryotes have two homologs of CAP, CAP1 and CAP2, which are closely related. CAP1 has been well studied [5, 13]. It is expressed in nearly all cells and organs of the mouse and is highly abundant [5]. At the subcellular level, it is present in regions with high actin dynamics. CAP2 has been less well studied. We have generated polyclonal antibodies specific for CAP1 and CAP2 and analyzed their distribution. We found that CAP2 is present only in a limited number of tissues and that it has a unique distribution at the subcellular level. During myogenesis, CAP2 is mainly a nuclear protein; in the adult muscle it is an M-band protein. In skin-derived cell lines, CAP2 is primarily a nuclear protein, and in skin it is a nuclear protein and also present at cell borders.

Materials and methods

Cloning of murine CAP1 and CAP2 cDNA, expression of recombinant protein and production of antibodies. CAP1 cDNA was amplified from mRNA derived from C3H10T1/2 cells, CAP2 cDNA was amplified from mRNA isolated from mouse heart. Primers used for CAP1 were: forward primer 5′-GTCGACATGGCTGACATGCAAAATCTT-3′, reverse primer 5′-GCGGCCGCTTATCCAGCGATTTCTGTCACT-3′; and for CAP2, forward primer 5′-GTCGACATGACAGACATGGCGGGACTG-3′ and reverse primer 5′-CGGCCGCTCAGGCCATGATCTCTGCAG-3′ (Sigma). CAP1 was expressed as a full-length protein using pT7–7 [14] and purified by cation exchange chromatography. For CAP2, GST-tagged polypeptides encompassing the N and the C terminus were expressed. To amplify the C-domain of CAP2, forward primer 5′-GTCGACGCTTTATTTCCCAGCTCAAT-3′ and reverse primer 5′-GCGGCCGCTCAGGCCATGATCTCTGCAG-3′ were used (Sigma). For F-actin interaction studies [3], the C-terminal domain of mouse CAP2 ($CAP2_{650}$) encompassing residues 261–476 was used either as a GST fusion protein or after release from GST by thrombin cleavage. GST fusion proteins were released by 20 mM glutathione in 100 mM Tris-HCl, pH 8.0. Proper folding of the polypeptides was checked and shown by NMR spectroscopy. For the generation of CAP1-specific polyclonal antibodies, recombinant full-length CAP1 was used; for the production of CAP2-specific polyclonal antibodies a N-terminal his-tagged polypeptide encompassing residues 1–207 was used ($CAP2_{NT}$). Primers used to amplify the N-domain were 5′-GTCGACGCTTTATTTCCCAGCTCAAT-3′ and 5′-GCGGCCGCTTTGCTCCAAGTGAGGCCTGT-3′ (Sigma). The antibodies were raised in rabbits and affinity purified using recombinant protein bound to nitrocellulose membranes (Schleicher and Schüll). After several washing steps with PBS the antibodies were eluted with 0.5 M acetic acid followed by immediate neutralization with 1 M Tris. BSA was added for stabilization (2 mg/ml). They were tested for specificity using CAP1 and CAP2 expressed as GFP-tagged fusion proteins in COS7 cells. They did not cross-react with full-length GFP-CAP2 or CAP1, respectively; however, they recognized the corresponding proteins in mouse and human tissues.

Mammalian cell culture. Cell lines were cultured as described previously [15], and transfections were done as described [16, 17]. PAM212 cells [18] were cultured in tissue culture dishes (Falcon) in DMEM (Gibco) supplemented with Chelex-100 (Bio-Rad)

treated 10 % heat-inactivated fetal calf serum, 1 mM pyruvate, 2 mM glutamine, 50 µg/ml streptomycin, 50 units/ml penicillin and 0.05 mM $CaCl_2$ (low calcium medium). HL-1 cells [19] were plated onto fibronectin-gelatin-coated plates or coverslips and cultured in Claycomb medium supplemented with 10 % fetal bovine serum, 100 units/ml penicillin, 100 µg/ml streptomycin, 0.1 mM norepinephrine, and 2 mM L-glutamine. C2F3 cells were grown in DMEM supplemented with 10 % fetal calf serum, 2 mM glutamine, 100 units/ml penicillin and 1 mg/ml streptomycin (Life Technologies, Eggenstein, Germany) in 5 % CO_2 at 37 °C. To induce differentiation, C2F3 mouse myoblast cells were grown on coverslips overnight with normal growth medium and the medium was then changed to differentiation medium (growth medium supplemented with 2 % horse serum) to induce differentiation. Cells were fixed at days 0–6. Isolation and culture of mouse skin primary cells was done as described [20]. Detection of CAP1 and CAP2 in immunoblots was done with affinity-purified polyclonal antibodies using appropriate dilutions followed by incubation with goat anti-rabbit IgG coupled to horseradish peroxidase (Sigma-Aldrich). Detection was by enhanced chemiluminescence and exposure to X-ray films.

Extraction of CAP2 from nuclei. Cultured cells were trypsinized, counted and washed once in PBS. They were resuspended in buffer 1 (0.32 M sucrose, 10 mM Tris, pH 8.0, 3 mM $CaCl_2$, 2 mM magnesium acetate, 0.1 mM EDTA, 0.5 % NP40, 1 mM DTT, 0.5 mM PMSF; 1×10^7 cells/400 µl buffer) and sonicated on ice (Sonicator UP200S, Dr. Hielscher, Berlin, Germany; 40 s, amplitude 50 %, cycle 0.5). This step was repeated until no more intact cells were observed by light microscopy. The resulting homogenate was centrifuged at 500 *g* for 5 min, washed twice in 1 ml buffer 1 without NP40 and centrifuged again. The resulting pellet contains purified nuclei. For partial extraction of the nucleoplasm according to [15], nuclei were resuspended in buffer 2 (20 mM HEPES, pH 7.9, 1.5 mM $MgCl_2$, 20 mM KCl, 0.2 mM EDTA, 25 % glycerine, 0.5 mM DTT, 0.5 mM PMSF; nuclei of 10^7 cells/30 µl buffer) and incubated on ice for 30 min. An equal volume of buffer 3 was added [20 mM HEPES, pH 7.9, 1.5 mM $MgCl_2$, 800 mM KCl, 0.2 mM EDTA, 25 % glycerine, 0.5 mM DTT, 0.5 mM PMSF, 1 % NP40, protease inhibitor cocktail (Sigma)] and the solution was incubated with shaking for further 30 min on ice. The solution was then centrifuged for 15 min at 14 000 *g*, the resulting supernatant was used as nucleoplasm, and the pellet was washed once and adjusted to an equal volume with PBS. Nucleoplasm and nuclear pellet were subjected to SDS-PAGE and Western blotting.

Fractionation of nuclei and sequential extraction. Nuclear fractionation followed by sequential extraction was done according to [21]. Briefly, cells were harvested after washing twice with ice-cold cytoskeletal (CSK) buffer (10 mM Pipes, pH 6.8, 100 mM NaCl, 300 mM sucrose, 1 mM $MgCl_2$, 1 mM EGTA, 1 mM DTT), and once with CSK supplemented with 0.1 mM ATP and complete protease inhibitor cocktail (Roche). Cell suspensions were supplemented with 1 mM PMSF. To separate the subcellular components into detergent-soluble and detergent-resistant fractions, cells were diluted twofold with CSK (including ATP and protease inhibitors) supplemented with 0.2 % Triton X-100, incubated on ice for 5 min, then fractionated by centrifugation at 4000 *g* for 1 min. The pelleted fraction was resuspended in CSK for extraction with NaCl. Sequential extractions with increasing NaCl concentrations from 0.2 to 2 M were carried out in CSK containing ATP, protease inhibitors and 0.1 % Triton X-100.

Tissue preparation and Western blotting. Mouse myofibrils were obtained as described [22, 23], and tissues were prepared as described [15]. For analysis of brain tissue by immunoblotting samples were frozen in liquid nitrogen and total protein extracts were prepared in 10 mM Tris-HCl, pH 7.8, 1 mM EGTA, 1 mM DTT, 0.5 mM PMSF containing complete mini protease inhibitor cocktail. After pelleting of the cell debris, supernatants were subjected to standard SDS-PAGE (10 % acrylamide) and proteins were blotted to nitrocellulose membrane.

Immunohistochemistry and immunofluorescence. Affinity-purified CAP2-specific polyclonal antibodies and monoclonal antibodies (mAbs) against Nesprin-2 [16] were used for staining of 10-µm cryosections according to standard protocols. For myomesin detection mAb BB78 was used (kind gift of D. Fürst, Bonn), mouse anti-emerin was from Novacastra Laboratories. Desmin, tropomyosin, α-actinin, myosin heavy chain for skeletal muscle, Lap2α antibodies were from commercial sources. Secondary antibodies for indirect immunofluorescence analysis were conjugated with Cy3 (Sigma), FITC (Sigma), Alexa 488, Alexa 568 (Molecular Probes) and Cy5 (Chemicon). F-actin was detected with TRITC-labeled phalloidin (Sigma) and nuclear staining was visualized with the DNA-specific dye DAPI (Sigma). Immunofluorescence of cultured cell lines was done as described [16]. Fixation was done with 3 % paraformaldehyde followed by Triton X-100 (0.5 %) treatment. Drug treatment was done with 2.5 µM latrunculin A, 2 µM cytochalasin D and 12.5 µM colchicin (Sigma) for the indicated time points. Microtubules were visualized

using tubulin-specific mAb WA3 (kind gift of Dr. U. Euteneuer, München). For microtubule staining fixation was done at room temperature in pre-cooled (4 °C) microtubule stabilization buffer (80 mM Pipes, pH 6.8, 1 mM $MgCl_2$, 1 mM EGTA, 0.5 % Triton X-100) for 1 min followed by chilled methanol (–20 °C) fixation for 5 min. Specimens were analyzed by wide-field fluorescence microscopy (DMR, Leica) or confocal laser scanning microscopy (TCS-SP, Leica). Image processing was done with Adobe Photoshop or the TCSNT software, respectively.

Effect of *Agaricus bisporus* lectin, and leptomycin B on nuclear import and nuclear export of CAP2. PAM212 cells were cultured overnight on glass coverslips in 24-well plates in growth medium. The cells were washed once with PBS. *Agaricus bisporus* lectin (ABL; from 0 to 80 μg/ml, diluted in growth medium; Sigma) was added, the same volume of diluent (PBS) was added to control cells, and then cells were cultured at 37 °C for 6 h. Then cells were washed twice with PBS and subjected to immunofluorescence. Similarly, overnight grown PAM212 cells on coverslips were washed once with PBS and treated with leptomycin B (LMB; 10 ng/ml; Sigma) for 60 and 90 min, washed twice with PBS and used for immunofluorescence.

Miscellaneous methods. Total RNA was isolated from various tissues of 8-week-old BALB/c mice [24]. For CAP2 mRNA detection in Northern blots, a probe encompassing nucleotides 1–634 (corresponding amino acid residues 1–211) of the cDNA was used, and for CAP1 mRNA detection a full-length cDNA was used. Actin was purified from chicken muscle following routine procedures including a gel filtration on Sephacryl S300 [25]. Low-shear viscometry, labeling of actin with *N*-(1-pyrenyl)iodoacetamide, and fluorescence spectroscopy of actin polymerization kinetics or the interaction between pyrenylated G-actin and $CAP2_{650}$ were done essentially as described [26]. When a GST-fusion of $CAP2_{650}$ was used, the experiments were also carried out with GST protein only to exclude that the GST-tag had an effect in the assays. In all cases these control experiments did not show any interaction of GST with actin. A human mRNA tumor array was purchased from BioChain Institute (Hayward, CA, USA; cat. no. H3235713).

Results

Comparison of the CAP1 and CAP2 amino acid sequences and tissue distribution. Mammalian CAP1 and CAP2 are highly related proteins. Mouse CAP2 shares 62 % identity and 76 % similarity with mouse CAP1. CAP1 and CAP2 from various mammalian species are 93–96 % (CAP1) and 88–93 % (CAP2) identical among each other and are equally distant to CAPs from non-mammalian species showing 33–34 % identity each to CAP/Srv2 from *S. cerevisiae* (Fig. 1a, b). The degree of homology between mouse CAP1 and CAP2 varies within the domains. It is slightly higher in the C-terminal domain than in the proline-rich central domain and the N-terminal domain. The N-terminal CAP-signature motif LxxRLE/DxxxxRLE comprising a leucine-rich stretch is conserved in CAPs from all species. In CAP2, the leucine-rich stretch is even more highly conserved and is extended to LxxRLExAVxRLExL (Fig. 1a).

The tissue distribution of CAP1 and CAP2 differs with CAP1 being more widely distributed than CAP2. Northern blot analysis revealed that the CAP1 gene is transcribed in all tissues examined and particularly well in testis, lung and kidney giving rise to a 2.5 kb mRNA (Fig. 2a), whereas the two CAP2-specific mRNAs of approximately 3 and 3.5 kb are strongly expressed in skeletal muscle, heart and testis (Fig. 2a). In RNA isolated from other tissues, e.g. liver, only weak or no signals are seen. For an analysis of CAP1 and CAP2 distribution at the protein level, we generated polyclonal antibodies using bacterially expressed full-length CAP1 and a polypeptide corresponding to the N-terminal domain of CAP2 (amino acids 1–207) as antigen. In Western blots, the antibodies recognized endogenous and GFP-tagged CAP2 expressed in COS7 cells, but not GFP-tagged CAP1 (Fig. 2b), whereas the CAP1 antibodies were specific for CAP1 and recognized an approximately 54-kDa protein in homogenates of COS7 cells and GFP-tagged CAP1, but not GFP-tagged CAP2.

CAP1 was recognized in homogenates of all tissues with the exception of muscle, where only a very faint signal was detected (Fig. 2c). CAP2 was detected in homogenates from brain, skin, heart, testis and in skeletal muscle as a protein of approximately 53 kDa (Fig. 2d). The cell lines that we tested by Western blot analysis (COS7, HEK293, A431) expressed CAP1; however, none of them showed significant CAP2 amounts (data not shown). We also did not detect CAP2 mRNA by the more sensitive RT-PCR technique in these cell lines (data not shown). Only PAM212 cells, a mouse keratinocyte cell line [18], showed a strong signal, whereas A431 cells, which are derived from a human skin carcinoma, were negative for CAP2. We consistently observed a faint 53-kDa signal in HEK293 cells (data not shown).

Localization of CAP2 in skeletal and cardiac muscle. To determine the subcellular distribution of CAP2 in striated muscle tissue, we analyzed human skeletal

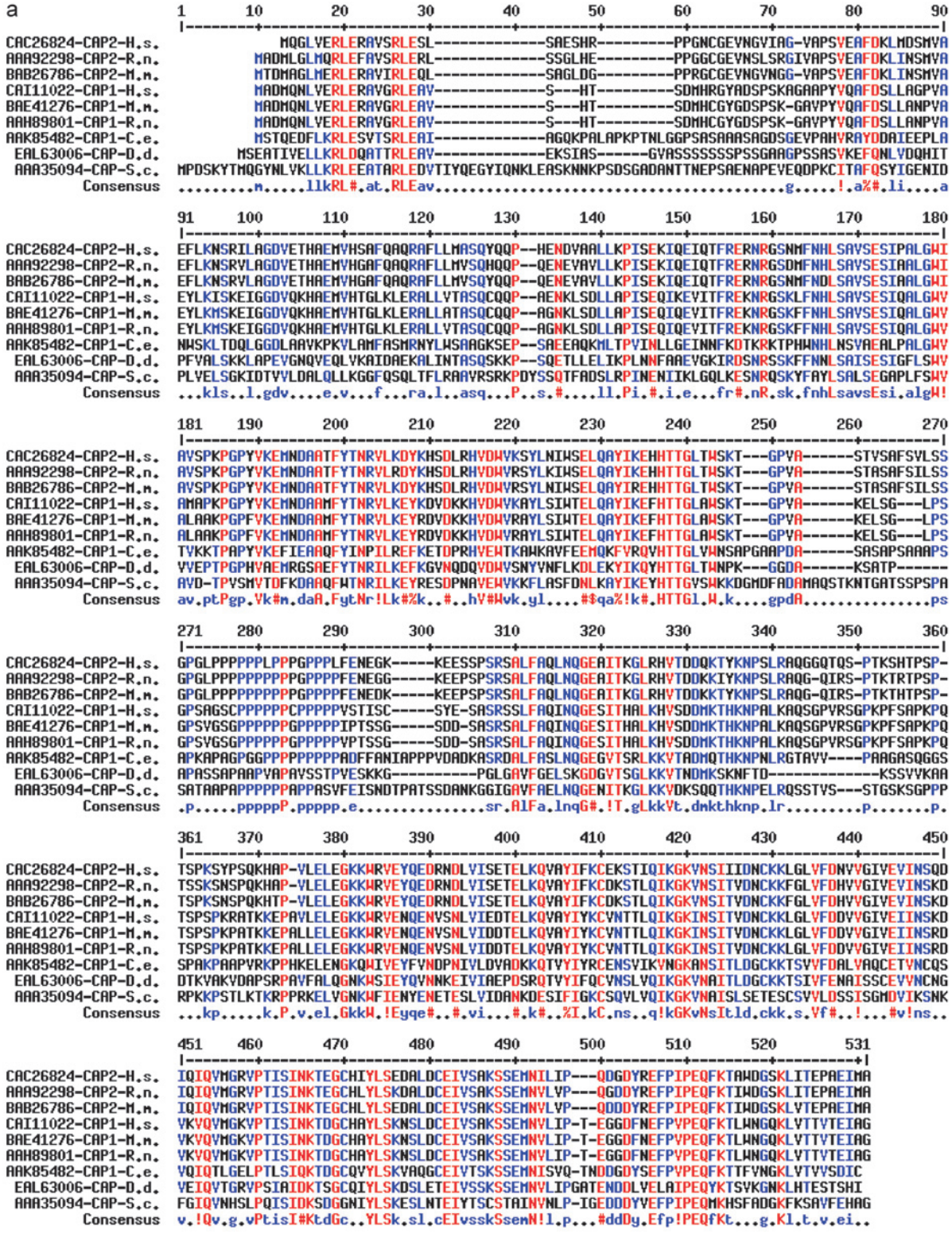

Figure 1. Comparison of cyclase-associated protein (CAP) sequences from various species. (*a*) Sequence comparison of CAP from different species using the multalin computer program. *Homo sapiens* (H.s.), *Rattus norvegicus* (R.n.), *Mus musculus* (M.m.), *Caenorhabditis elegans* (C.e.), *Dictyostelium discoideum* (D.d.) and *Saccharomyces cerevisiae* (S.c.). CAP sequences were used for the alignment. The accession numbers are indicated at the front of individual gene name. High consensuses are shown in red, while low and neutral consensuses are shown in blue and black, respectively. Consensus symbols are "!", I or V; $, L or M; %, F or Y, #, any one of N, D, Q, E. (*b*) Sequence comparison of CAP from different organisms by Clustal W shown as a dendrogram. CV, *Chlorohydra viridissima*, CE, *C. elegans*, LE, *Lentinula edodes*, CA, *Candida albicans*, SC, *S. cerevisiae*, SP, *Schizosaccharomyces pombe*, DD, *D. discoideum*, AT, *Arabidopsis thaliana*, GH, *Gossypium hirsutum*, DM, *Drosophila melanogaster*, HS, *H. sapiens*, MM, *M. musculus*, RN, *R. norvegicus.*

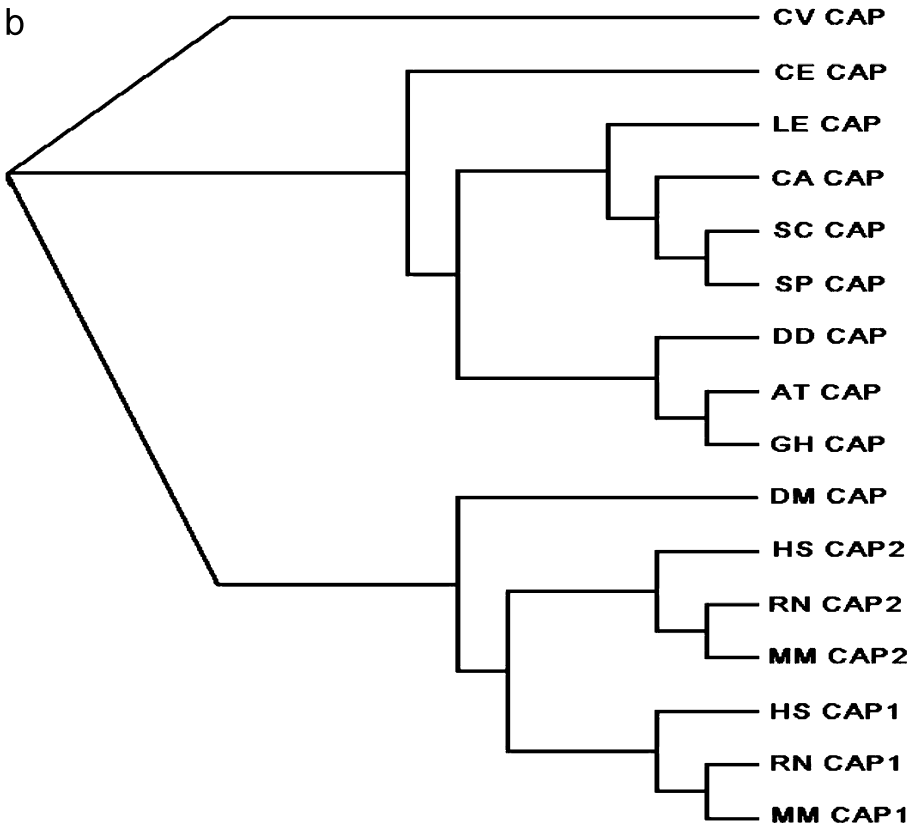

Figure 1. *(continued)*

and mouse cardiac muscle. CAP2 immunostaining of cross-sectioned human skeletal muscle showed a sarcoplasmic staining pattern in both type I and type II fibers (Fig. 3a and data not shown), whereas the analysis of longitudinal sections revealed a cross-striated staining pattern (Fig. 3a). In contrast, sarcolemmal or nuclear staining was not observed. Double-immunofluorescence analysis with antibodies recognizing desmin, which is located at the Z-bands, clearly showed that CAP2 does not localize at the Z-band (Fig. 3b). A cross-striated staining pattern was also observed in our analysis of myofibrils isolated from heart. In double-immunofluorescence studies with antibodies against CAP2 in conjunction with antibodies against α-actinin (Z-band marker), troponin I (A-band marker) and myomesin (M-band marker), the position of CAP2 overlapped with the one of myomesin but not with the one of α-actinin and troponin I (Fig. 4a–c). Myomesin is a constituent of the M-line located in the middle of the A-band. These findings indicate that CAP2 is a component of myofibrillar M-bands. In addition to the strong M-band staining, we noted a faint line between two M-bands, which might be the neighboring I-bands.

In embryonic cardiomyocytes (days 17 and 19), CAP2 localized to the nucleus and was diffusely present in the cytoplasm. Troponin I, which was tested for control, exhibited a cytoplasmic distribution similar to the one of CAP2 (data not shown). In HL-1 cells, a cardiac muscle cell line [19], CAP2 was also present in nuclei (data not shown). These findings suggested to us that CAP2 might change its localization during myogenesis. We therefore used the myogenic cell line C2F3 in which myogenesis can be induced by starvation. In undifferentiated C2F3 cells, CAP2 is almost exclusively found in the nucleus. Upon differentiation, it accumulates in the cytosol and the nuclear staining becomes less intense. To test for differentiation, we followed the expression of skeletal myosin heavy chain, which is only expressed in differentiating C2F3 cells (Fig. 5).

CAP2 is a dual compartment protein. In our analysis of CAP2 presence in various cell lines, we identified the mouse keratinocyte cell line PAM212 as being strongly positive for CAP2. The immunofluorescence analysis revealed that CAP2 is present in the nuclei of the majority of the cells. In addition, we observed a weak staining of the cytoplasm (Fig. 6a). CAP1 is also expressed in PAM212 cells allowing a direct comparison of the localization of both proteins. CAP1 proved to have a completely different distribution. It was diffusely present in the cytoplasm and did not localize to the nucleus (Fig. 6a).

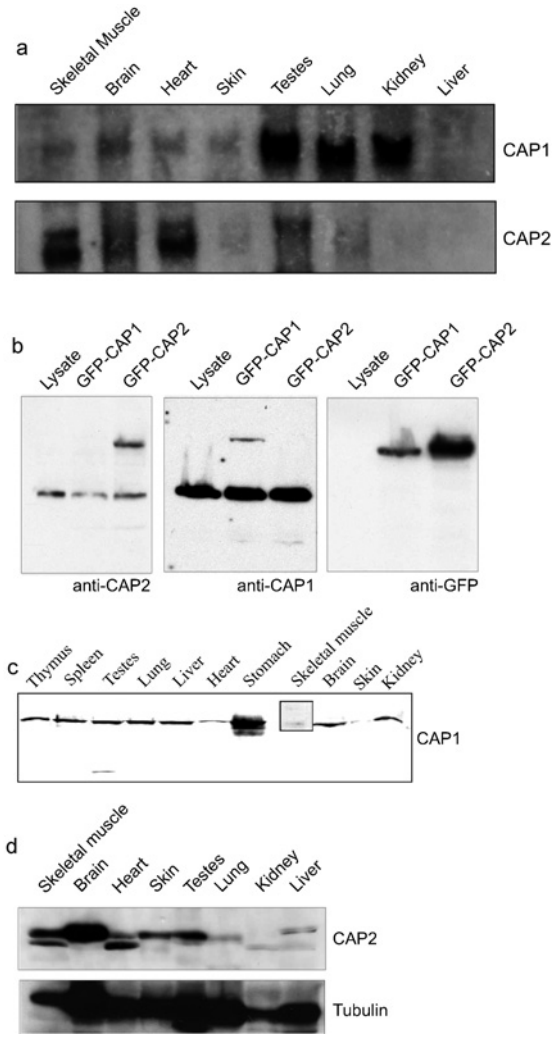

Figure 2. Distribution of CAP in tissues. (*a*) Presence of CAP2 transcripts in various tissues. RNA (20 µg) from different tissues (skeletal muscle, brain, heart, skin, testes, lung, kidney and liver) of an adult mouse was separated on a 1 % agarose gel in the presence of formaldehyde. The resulting blot was probed with a probe corresponding to full-length mouse CAP1 cDNA, and subsequently with a probe corresponding to nucleotides 1–634 of the mouse CAP2 cDNA. (*b*) Specificity of CAP1 and CAP2 polyclonal antibodies. Homogenates of COS7 cells and COS7 cells expressing GFP-tagged CAP1 or GFP-CAP2 were separated by SDS-PAGE (12 % acrylamide). The blot was probed with polyclonal antiserum (1:5000) raised against CAP2 followed by chemiluminescence. The blot was stripped and reprobed with CAP1-specific antiserum (1:1000). The blot was then stripped again and reprobed with GFP-specific mAb K3–184–2 recognizing the GFP-fusion proteins. The CAP2-specific antibodies reacted only with CAP2 proteins and did not detect GFP-CAP1, and CAP1-specific antibodies detected only GFP-CAP1 but not GFP-CAP2. Lower bands indicate the respective endogenous CAP1 and CAP2. (*c*) Presence of CAP1 in mouse tissues. Homogenates from thymus, spleen, testis, lung, liver, heart, stomach, skeletal muscle, brain, skin, kidney were probed for CAP1 presence. To detect a signal in skeletal muscle, the blot had to be exposed to the film for an extended period of time. (*d*) Presence of CAP2 in mouse tissues. Homogenates of adult mouse skeletal muscle, brain, heart, skin, testes, lung, kidney and liver were separated by SDS-PAGE (10 % acrylamide) and the blots probed for CAP2 presence. Tubulin was used for control.

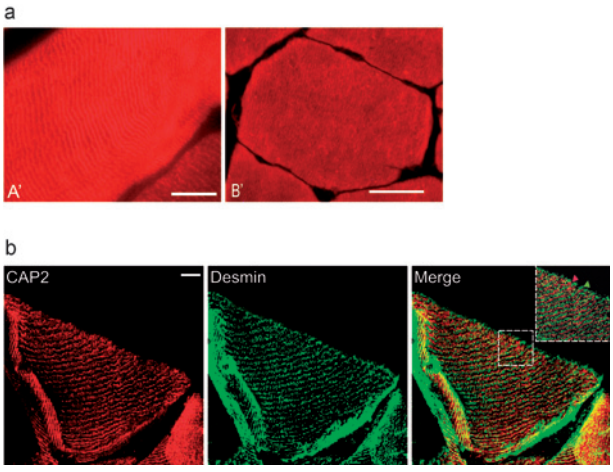

Figure 3. (*a*) CAP2 immunostaining of normal human skeletal muscle using CAP2-specific polyclonal antibodies. (*A′*) Analysis of longitudinal sections showed a cross-striated staining pattern. Bar, 15 µm. (*B′*) Analysis of cross-sections revealed a sarcoplasmic staining pattern. Bar, 20 µm. (*b*) Adult human muscle section was stained with CAP2-specific polyclonal antibodies and co-stained with desmin specific mAbs, respectively. Detection was with secondary anti-rabbit IgG antibody conjugated to Alexa 568 and a secondary anti-mouse antibody conjugated to Alexa 488. The arrows in the inset point to desmin and to CAP2-stained structures, respectively.

We confirmed the presence of CAP2 in the nucleus by cell fractionation experiments. CAP2 was strongly enriched in the nuclear membrane fraction (2000-rpm pellet), which contains nuclei, and also in the 12 000-rpm pellet and supernatant. Emerin, a protein of the nuclear membrane that was used for control was present in the 2000-rpm pellet (data not shown). We further tested the extractability of CAP2 from nuclei. In this experiment CAP2 behaved like emerin and could not be extracted from nuclei and stayed in the pellet after extraction with a hypotonic extraction buffer that was used to obtain the nucleoplasm and nuclear pellet. As a further control, we probed the same blot with Lap2α (non-membrane-bound isoform of Lap2) and tubulin-specific antibodies as markers of nucleoplasm and cytoplasm, respectively. LAP2α was present in the nucleoplasm, emerin and CAP2 were found in the nuclear pellet, and tubulin was only detected in the lysate (Fig. 6b).

The interaction of proteins with structural components of the nucleus has been well studied previously using high salt treatments that solubilize most of the proteins in the nucleus. The resistant fractions are classified as nuclear matrix proteins (reviewed in [27]). We applied a similar technique in which we treated nuclei with increasing amounts of salt. We found that CAP2 is tightly bound and is released from the nucleus primarily by adding 2 M NaCl (Fig. 6c). This indicates that the detergent-resistant CAP2 is immobilized by attachment to non-chromatin struc-

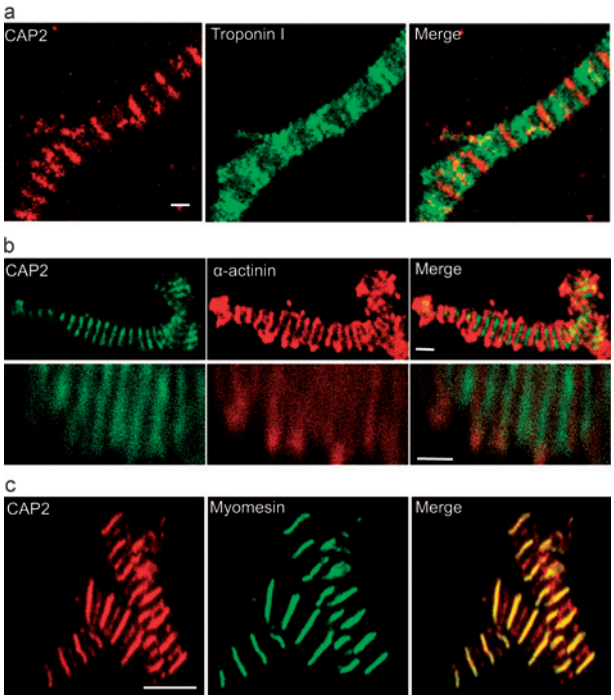

Figure 4. CAP2 in heart muscle. (*a*) Myofibrils were stained with CAP2-specific polyclonal antibodies and cardiac-specific anti-troponin I mAbs. Detection was with secondary anti-rabbit IgG antibody conjugated to Alexa 568 and a secondary anti-mouse antibody conjugated to Alexa 488. (*b*) Myofibrils were stained with CAP2-specific polyclonal antibodies and α-actinin mAbs. Detection was with secondary anti-rabbit IgG antibody conjugated to Alexa 488 and a secondary anti-mouse antibody conjugated to Alexa 568. (*c*) CAP2 localizes to the M-band in myofibrils. Myofibrils were co-stained with CAP2-specific polyclonal antibodies and an mAb recognizing myomesin. In addition to the strong M-band staining by the CAP2 antibodies, a faint line between two M-bands is seen which might correspond to the I-band. Detection was with secondary anti-rabbit IgG antibody conjugated to Alexa 568 and a secondary anti-mouse antibody conjugated to Alexa 488. Confocal images are shown. Bar, 2.5 μm for (*a*) and (*c*), 3 μm for (*b*).

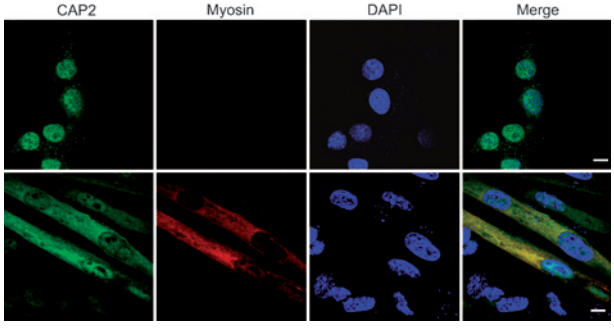

Figure 5. Localization of CAP2 during myoblast differentiation. C2F3 mouse myoblast cells were changed from growth medium to medium containing 2% horse serum to induce differentiation. Staining was with CAP2-specific polyclonal antibodies and skeletal muscle myosin mAbs. Detection was done with secondary anti-rabbit IgG antibody conjugated to Alexa 488 and a secondary anti-mouse antibody conjugated to Alexa 568. Bar, upper panel, 10 μm; lower panel, 8 μm.

tures, but this does not rule out associations with DNA or chromatin in addition to non-chromatin structures, which would not be revealed by this experiment. In contrast, the majority of Annexin A7, which is also present in the nucleus [15], was released by low concentrations of salt; some residual protein is also released by 2 M NaCl (Fig. 6c).

To determine whether or not nuclear import and nuclear export of CAP2 is dependent on a functional nuclear localization signal (NLS) and nuclear export signal (NES), the edible mushroom (*A. bisporus*) lectin ABL, and LMB, an antifungal agent, were used as inhibitors of NLS-dependent import and NES-dependent export, respectively [28, 29]. We found no alteration of nuclear localization of CAP2 under these conditions (data not shown). These results indicate that nuclear export of CAP2 is not mediated through the CRM1 receptor.

As a nuclear localization of CAP2 was also observed in primary keratinocytes (data not shown), we extended our studies to human skin sections. CAP2 is present in all living layers of the epidermis. The CAP2 antibodies strongly stain the cell periphery (arrowheads in Fig. 7) and the nucleus (arrows in Fig. 7). Higher magnification reveals a dotted staining pattern at the cell periphery (Fig. 7f), and co-staining with Nesprin-2-specific antibodies reveals CAP2 localization inside the nucleus (Fig. 7d, e). Nesprin-2 is an actin-binding protein of the nuclear membrane and primarily stains the nuclear envelope [30].

CAP2 association with the cytoskeleton. CAPs from lower and higher eukaryotes have been shown to influence F-actin dynamics and bind to G-actin. An actin association of CAP2 has not been addressed so far as the insolubility of recombinant full-length CAP2 or its C-terminal domain prevented a direct assessment of the actin interaction. We therefore tested the effect of the microfilament-disrupting drug latrunculin B and cytochalasin D on the CAP2 distribution in PAM212 cells. Untreated cells have an intact actin cytoskeleton, and stress fibers extend throughout the cells. CAP2 is mainly present in the nucleus; the cytosol exhibits a weak and diffuse CAP2 staining. In latrunculin B-treated cells, the stress fibers have disappeared; instead, a diffuse staining is seen and at later time points actin clumps have formed. By contrast, CAP2 localization is not affected by latrunculin B treatment. Nuclear localization is also not affected by disruption of the actin cytoskeleton with cytochalasin D. It remains in the nucleus throughout the experiment, and the diffuse cytosolic staining is unaltered as well (Fig. 8a, b). We also tested the effect of colchicin, which destroys the microtubule network, on CAP2 distribution. As for latrunculin and cyto-

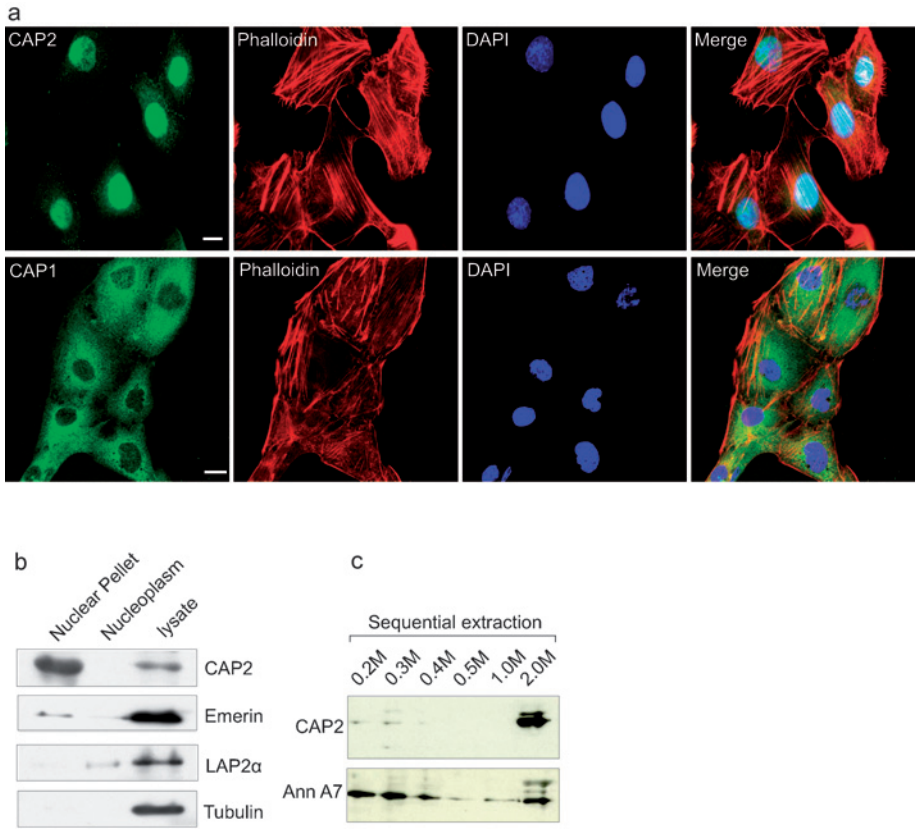

Figure 6. CAP1 and CAP2 have a different subcellular localization in PAM212 cells. (*a*) PAM212 cells were stained with CAP2 (upper panel) and CAP1 (lower panel) specific antibodies. F-actin was visualized by TRITC-conjugated phalloidin, nuclei were stained with DAPI. Bar in upper panels, 12.5 μm; bar in lower panels, 15.8 μm. (*b*) Extraction of CAP2 from nuclei of the mouse keratinocyte (PAM212) cell line using a hypotonic buffer. Samples of total cells (lysate), and corresponding amounts of nuclear pellet and nucleoplasm were subjected to SDS-PAGE and Western blotting. CAP2 remains in the pellet fraction that also contains the nuclear membranes. For control, immunoblotting of LAP2α (non-membrane-bound isoform), emerin, and tubulin, which are specific for nucleoplasm (LAP2α), nuclear membranes (emerin), and the cytoplasm (tubulin) are shown. (*c*) Sequential extraction using increasing amounts of NaCl concentrations indicates a tight association of CAP2 with the nuclear matrix, whereas Annexin A7 is only loosely bound.

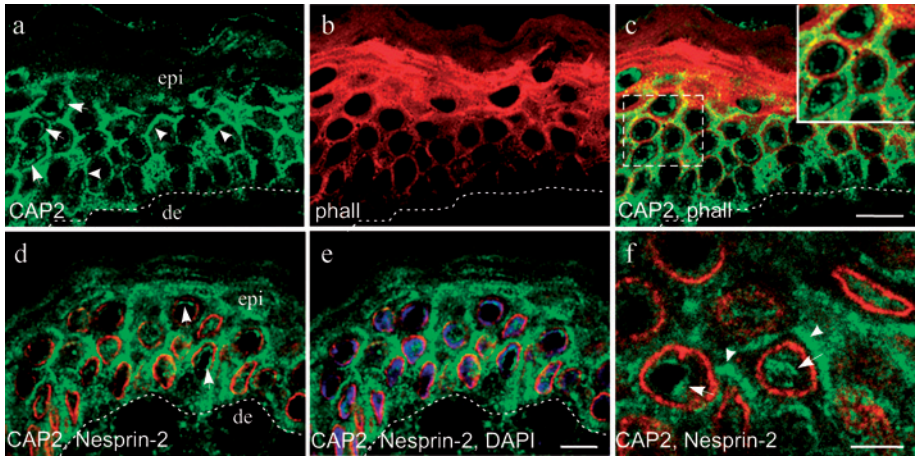

Figure 7. CAP2 localizes in human skin at cell-cell borders and in the nucleus. (*a–c*) Human 10-μm frozen skin sections were stained with anti-CAP2-specific antibodies and TRITC-conjugated phalloidin to visualize the cell periphery. Arrowheads indicate staining at the cell periphery, whereas arrows indicate nuclear staining. Inset in (*c*), is a higher magnification of the white dotted boxed area. (*d–f*) Human skin sections stained with anti-CAP2 and anti-Nesprin-2 antibodies (*d*, *f*) as well as DAPI (*e*) to reveal the nuclear presence of CAP2. Note that, in contrast to the nuclear envelope Nesprin-2 localization, the CAP-2 staining is confined within the nucleus (arrows) and at cell borders (arrowheads). The dotted lines denote the basement membrane. DNA was stained with DAPI. Images were taken by confocal microscopy. epi, Epidermis; de: dermis. Bars in (*c*, *e*) 10 μm, (*f*) 5 μm.

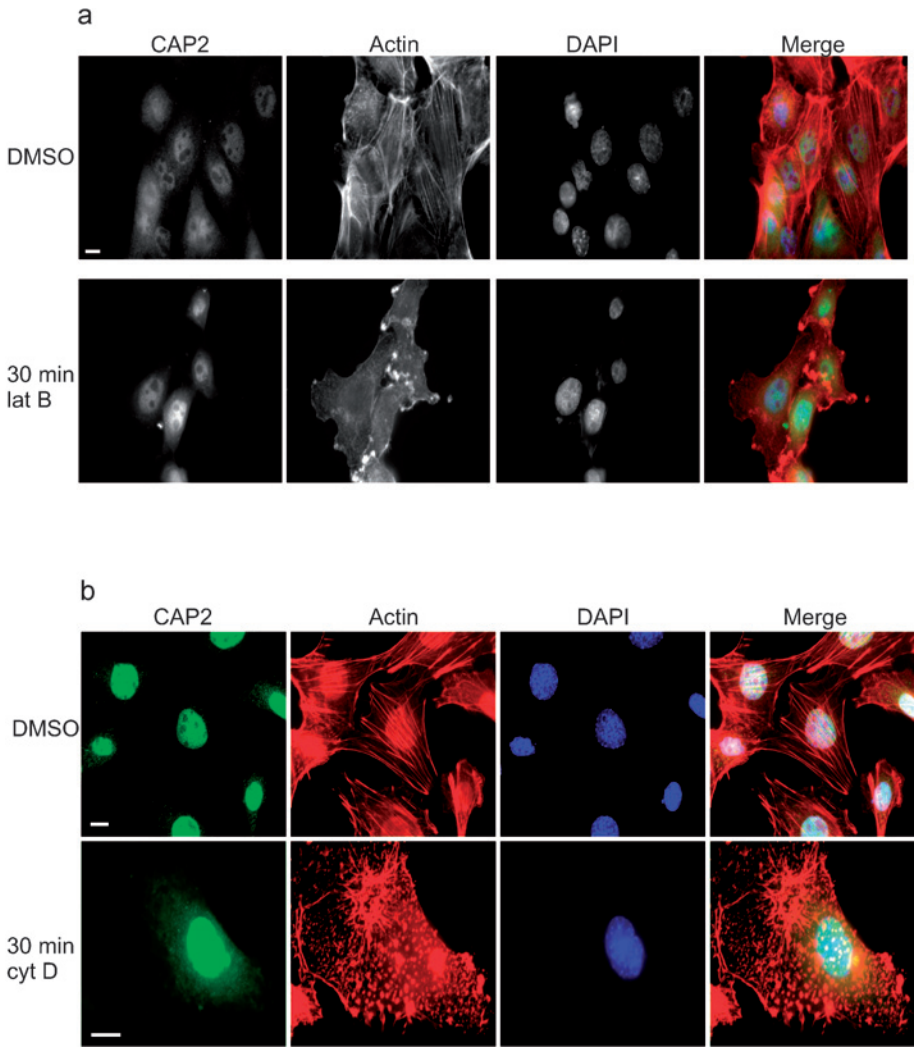

Figure 8. CAP2 localization in PAM212 cells is not influenced by latrunculin B (lat B) and cytochalasin D (cyt D) treatment, drugs that disrupt the actin cytoskeleton. PAM212 cells were treated with latrunculin B (2.5 μM) or with cytochalasin D (2 μM) for various periods of time and stained for CAP2 with polyclonal antibodies. F-actin was visualized by TRITC-phalloidin, nuclei were stained with DAPI. Bar in (*a*) 10 μm; (*b*) lower and upper panel, 18.5 μm.

chalasin treatment, CAP2 distribution was not affected (data not shown).

We then tested for an interaction between actin and CAP2 *in vitro*, and observed effects in the fluorescence enhancement of pyrene-labeled G-actin, in actin polymerization and in low-shear viscometry assays. For these experiments, we used the C-terminal domain of CAP2, $CAP2_{650}$. This polypeptide encompasses amino acids 261–476, which comprise the region that has been proposed to be required for the actin interaction of various CAPs. $CAP2_{650}$ contains the region that has homology to a WH2 domain, and includes a verprolin homology region [10] as well as a region for which the structure has been elucidated by crystallography for the yeast protein [12]. $CAP2_{650}$ led to an enhancement of the emission of pyrene-labeled G-actin with respect to the G-actin spectra, and increasing amounts led to an increase in the relative fluorescence (Fig. 9a). It is important to note that this assay was performed under strictly non-polymerizing conditions in low-salt G-actin buffer (2 mM Tris-HCl, 0.2 mM $CaCl_2$, 0.5 mM DTT, 0.2 mM ATP, pH 8.0). The fluorescence of pyrenylated G-actin is minuscule and requires highest sensitivity of the photomultiplier. However, an increase of this signal after addition of $CAP2_{650}$ shows clearly that both proteins (monomeric actin and $CAP2_{650}$) interact. In polymerization experiments using pyrene-labeled G-actin, the addition of $CAP2_{650}$ led to a delay in the polymerization (Fig. 9b), again indicative of a direct 1:1 interaction between monomeric actin and $CAP2_{650}$. In contrast to barbed-end capping proteins that also lead to a delay of polymerization, this effect occurs with $CAP2_{650}$ only at roughly equimolar concentrations. The 1:1 complex cannot polymerize, thus the concentration of polymerizable free actin is decreased, leading to a delayed formation of filaments. The same effect of $CAP2_{650}$ on actin polymerization was observed in low shear viscometry. When G-actin was polymerized in the presence of the protein the viscosity measured was

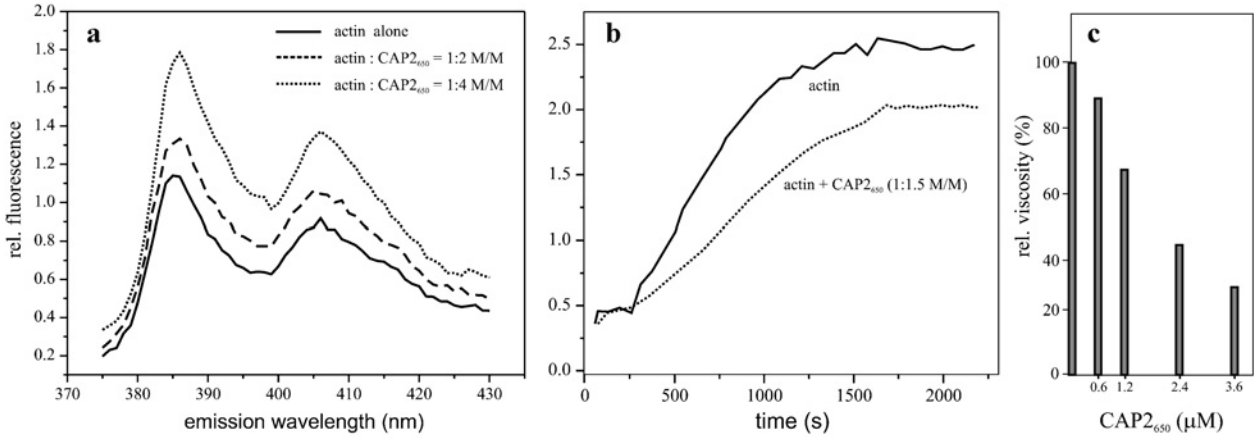

Figure 9. Interaction of CAP2 with actin. (*a*) An emission spectrum of pyrenylated G-actin in the absence or presence of GST-$CAP2_{650}$ at a molar excess of 1 : 2 or 1 : 4 shows an increase of the emitted signal, which suggests a direct binding of monomeric actin to $CAP2_{650}$. G-actin 5 μM containing 10 % pyrene-labeled actin were used in the assays. The excitation wavelength was 386 nm. (*b*) Polymerization of actin is inhibited in the presence of $CAP2_{650}$ at a molar ratio of 1 : 1.5 (3 μM actin: 4.5 μM $CAP2_{650}$). (*c*) The viscosity of an F-actin solution decreases with increasing concentrations of $CAP2_{650}$, due to the formation of a non-polymerizable 1 : 1 complex removing polymerizable G-actin from the G-/F-actin equilibrium (actin concentration: 8 μM).

Table 1. A human tumor mRNA array containing 47 pairs of tumor RNA samples was probed with a CAP2-specific probe (first 900 bp of the cDNA). Data show only the tumors in which CAP2 was significantly up- or down-regulated.

Tumor type	Normal	Tumor
Bladder tumor (transitional cell carcinoma level III)	+	+ + +
Colon tumor (adenocarcinoma well-differentiated)	+	+ + +
Thyroid tumor (adenocarcinoma)	–	+ + +
Kidney tumor (clear cell carcinoma)	–	+ +
Breast tumor (fibroadenoma)	+ + + +	Very low

reduced in a dose-dependent manner (Fig. 9c). All three assays show that the formation of actin gels is inhibited by an interaction of CAP_{650} with monomeric actin. The activity of CAP2 might, therefore, resemble the one of other CAPs [3].

CAP2 in cancer. To further analyze the CAP2 function, we extended our studies to a cancer array. It has been reported before that CAP2 is highly up-regulated in hepatocellular carcinoma, which is associated with chronic liver disease, known to show an obvious multistage process of tumor progression [31]. CAP2 regulation in other carcinomas remained unclear. Here we studied CAP2 regulation at the mRNA level for 47 different types of tumors. A human mRNA tumor array was used and the probe used in this experiment covered approximately the first 900 bp of cDNA. For control, actin cDNA was used. At the RNA level, we observed that CAP2 was highly up-regulated in bladder tumor (transitional cell carcinoma level III), colon tumor (adenocarcinoma well-differentiated) and thyroid tumor (adenocarcinoma). In normal kidney it is completely absent at the RNA level, while in kidney tumor (clear cell carcinoma) it is highly up-regulated. CAP2 was highly down-regulated only in breast tumor (fibroadenoma), while in brain tumor it was considerably up-regulated (Table 1). This leads us to conclude that CAP2 can be up- or down-regulated in cancer depending upon the type and its origin.

Discussion

CAP is considered an actin-binding protein and a loss of the protein or mutations in the gene in yeast, *D. discoideum* and *Drosophila* lead to defects in processes associated with the actin cytoskeleton. Most species have a single gene coding for CAP, mammals have two genes that code for closely related proteins, CAP1 and CAP2. The importance of two isoforms of CAP in mammals is not known. The interaction of CAP1 with G-actin has been well studied, and a role in the regulation of actin dynamics by affecting the ADP/ATP exchange on G-actin has been demonstrated [5, 13]. Furthermore, the C-terminal domain of CAP1 was identified as a primary G-actin binding site. In addition, the localization of CAP1 to regions of the

cells with high actin dynamics supports its role as protein regulating the actin cytoskeleton. In contrast, the role of CAP2 in regulating actin dynamics is unclear so far. The high sequence conservation suggests, however, that the function as G-actin binding protein might be conserved among all CAPs. This is underlined by the fact that the C-terminal domains of CAP show the highest conservation in the protein.

The structure of the actin binding C-domain has been solved for yeast CAP/Srv2 [12]. It contains an unusual β-helical structure whose core may represent the structural archetype for a wide range of proteins such as the RP2 protein, which is responsible for X-linked forms of retinitis pigmentosa, a disease characterized by retinal degeneration, and cofactor C. RP2 is a plasma membrane-associated protein of unknown function, which was recently described as a DNA-binding protein that exhibits exonuclease activity and that undergoes re-localization into the nucleus upon treatment of cells with DNA-damaging agents [32]. Its N-terminal domain shares amino acid sequence similarity to the C-terminal domain of CAP and to the tubulin-specific chaperone protein cofactor C. The tubulin-specific chaperone protein cofactor C is the GTPase-activating component of the tubulin folding complex, which is responsible for assembly of the tubulin heterodimer. Furthermore, this domain is present in many other uncharacterized proteins, suggesting that many signaling pathways utilize this cytoskeleton-related motif. The basic unit has been called CARP domain (cyclase-associated protein and X-linked retinitis pigmentosa 2 gene product, XRP2). CAPs have two CARP domains in tandem repeats. In mouse CAP2, they extend from amino acids 358 to 395 and from 396 to 433.

The structural data obtained for the C-domain of CAP do not allow the identification of the G-actin binding site in the molecule, as the residues that have been suspected to be involved in G-actin binding by yeast two-hybrid analysis (residues 499–526, [9]) are the ones that are involved in formation of the strand exchanged CAP dimer, so that conclusions for a potential CAP2-actin interaction cannot be drawn.

Inspection of the CAP2 protein sequence did not reveal any other motif. The results of our immunofluorescence studies were, therefore, surprising when they revealed that CAP2 is a dual compartment protein. In the mouse keratinocyte cell line PAM212, we found the endogenous protein primarily in the nucleus. In the skin, it was present in the nucleus and at cell-cell junctions. The latter situation resembles the one observed for β-catenin, which has a role in the formation of cell junctions as well as in signaling to the nucleus [33]. CAP2 is also strongly enriched in the nucleus in developing cardiomyocytes. It changes its localization in the adult cardiomyocyte and is then observed at the M-band. The M-band is an important element of the sarcomer, the elementary contractile unit of striated muscle. It is believed to maintain the thick filament lattice through interactions of the prominent M-band component myomesin, which links the thick filaments. Another component of the M-band is M-protein. The muscle isoform of creatine kinase is also located at the M-band; titin is situated at the M-band through its C terminus, with which it interacts with muscle-specific RING finger (MURF) proteins and with DRAL/FHL-2, a protein composed of 4 and ½ LIM motifs [34]. Interestingly, the FHL proteins have a nuclear shuttling activity in addition to their association with the cytoskeleton [35]. Nuclear cytoplasmic redistribution has also been reported for myopodin, another component of skeletal and heart muscle [36]. Myopodin binds to F-actin. In myoblasts it shows preferential nuclear localization; during myotube differentiation it binds to stress fibers and is subsequently incorporated into the Z-disc. Upon thermal stress, myopodin can shuttle back into the nucleus. Myopodin contains a nuclear localization signal and requires phosphorylation-dependent 14–3-3 binding for importin α binding and subsequent nuclear import [37]. By contrast, CAP2 does not contain predicted nuclear import or export motifs. Also, we could not interfere with its nuclear localization employing the commonly used inhibitors of nuclear import and export ABL and LMB, which indicates that CAP2 does not use CRM1 for nuclear export [28].

The availability of highly specific antibodies for CAP1 and CAP2 allowed a direct comparison. CAP1 and CAP2 differ widely in their tissue distribution. CAP1 is broadly expressed, whereas CAP2 shows a restricted pattern and is primarily found in brain, skeletal and cardiac muscle, and skin. These are tissues with reduced CAP1 staining. For example, CAP1 is hardly detectable in homogenates from skeletal muscle, whereas CAP2 could be readily detected in this tissue. CAP1 and CAP2 differ not only in their tissue distribution, but also in their subcellular distribution. This was particularly evident in PAM212 cells, which co-express both proteins. CAP1 localized to dynamic regions of the cortical actin cytoskeleton such as lamellipodia, whereas CAP2 was only present in the nucleus, and the cytosol exhibited a diffuse and rather weak staining.

When we used the recombinant C-terminal domain of CAP2 for analysis of an actin interaction *in vitro*, we observed an inhibitory effect on actin polymerization as described previously for CAP from lower eukaryotes and mammalian CAP1 [3, 5], making it likely that CAP2 interacts with monomeric actin *in*

vivo and regulates actin dynamics to a certain extent.

Apart from the presence of actin in the cytoplasm, many studies have established its presence in the nucleus and have shown that its functions in the nucleus are as diverse as in the cytoplasm [38, 39]. Actin was shown to be a component of RNA polymerase complexes and participate in RNA transcription as well as in chromatin remodeling and RNA processing [40]. In general, actin is not detected in the nucleus using phalloidin or actin-specific antibodies. This has been thought to be due to the existence of different actin conformations that are not recognized by conventional tools. Conformation-specific antibodies with which these problems can be solved are now available [41].

Not only is actin present in the nucleus but also many other proteins that react with conventional actin forms in the cytoplasm. These include the F-actin-binding proteins gelsolin, CapG, cofilin and the G-actin-binding proteins profilin and thymosin [42]. Recently, evidence has been provided that supports polymeric forms of actin in the nucleus as well [43]. How the dynamics of actin is controlled in the nucleus is an unsolved question. Nuclear actin binding proteins will certainly be important players in this game and one of them might be CAP2.

Acknowledgements. We thank Dr. W. C. Claycomb (LSU, New Orleans, LA) for the gift of HL-1 cells, Dr. S. Yuspa for PAM212 cells, S. Hilsdorf and D. Rieger for technical assistance, and Dr. A. Hasse for providing brain homogenates. This work was supported the DFG (No 113/14), SFB 413, by Köln Fortune and the Fonds der Chemischen Industrie.

1 Pollard, T. D. (2003) The cytoskeleton, cellular motility and the reductionist agenda. Nature 422, 741 – 745.
2 Freeman, N. L., Chen, Z., Horenstein, J., Weber, A. and Field, J. (1995) An actin monomer binding activity localizes to the carboxyl-terminal half of the *Saccharomyces cerevisiae* cyclase-associated protein. J. Biol. Chem. 270, 5680 – 5685.
3 Gottwald, U., Brokamp, R., Karakesisoglou, I., Schleicher, M., and Noegel, A. A. (1996) Identification of a cyclase-associated protein (CAP) homologue in *Dictyostelium discoideum* and characterization of its interaction with actin. Mol. Biol. Cell 7, 261 – 272.
4 Hubberstey, A. V. and Mottillo, E. P. (2002) Cyclase-associated proteins: Capacity for linking signal transduction and actin polymerization. FASEB J. 16, 487 – 499.
5 Bertling, E., Hotulainen, P., Mattila, P. K., Matilainen, T., Salminen, M. and Lappalainen, P. (2004) Cyclase-associated protein 1 (CAP1) promotes cofilin-induced actin dynamics in mammalian nonmuscle cells. Mol. Biol. Cell 15, 2324 – 2334.
6 Noegel, A. A., Rivero, F., Albrecht, R., Janssen, K.-P., Köhler, J., Parent, C. A. and Schleicher, M. (1999) Assessing the role of the ASP56/CAP homologue of *Dictyostelium discoideum* and the requirements for subcellular localization. J. Cell Sci. 112, 3195 – 3203.
7 Noegel, A. A., Blau-Wasser, R., Sultana, H., Müller, R., Israel, L., Schleicher, M., Patel, H. and Weijer, C. J. (2004) CAP/ASP56 as regulator of cell polarity and cAMP signaling in *Dictyostelium.* Mol. Biol. Cell 15, 934 – 945.
8 Lila, T. and Drubin, D. G. (1997) Evidence for physical and functional interactions among two *Saccharomyces cerevisiae* SH3 domain proteins, an adenylyl cyclase-associated protein and the actin cytoskeleton. Mol. Biol. Cell 8, 367 – 385.
9 Zelicof, V., Protopopov, V., David, D., Lin, X. Y., Lustgarten, V. and Gerst, J. E. (1996) Two separate functions are encoded by the carboxyl-terminal domains of the yeast cyclase-associated protein and its mammalian homologs. Dimerization and actin binding. J. Biol. Chem. 271, 8243 – 8252.
10 Ksiazek, D., Brandstetter, H., Israel, L., Bourenkov, G. B., Katchalova, G., Janssen, K.-P., Bartunik, H. D., Noegel, A. A., Schleicher, M. and Holak, T. A. (2003) Structure of the N-terminal domain of the adenylyl cyclase associated protein (CAP) form *Dictyostelium discoideum.* Structure 11, 1171 – 1178.
11 Mavoungou, C., Israel, L., Rehm, T., Ksiazek, D., Krajewski, M., Popowicz, G., Noegel, A. A., Schleicher, M. and Holak, T. A. (2004) NMR structural characterization of the N-terminal domain of the adenylyl cyclase-associated protein (CAP) from *Dictyostelium discoideum.* J. Biomol. NMR 29, 73 – 84.
12 Dodatko, T., Fedorov, A. A., Grynberg, M., Patskovsky, Y., Rozwarski, D. A., Jaroszewski, L., Aronoff-Spencer, E., Kondraskina, E., Irving, T., Godzik, A. and Almo, S. C. (2004) Crystal structure of the actin binding domain of the cyclase-associated protein. Biochemistry 43, 10628 – 10641.
13 Moriyama, K. and Yahara, I. (2002) Human CAP1 is a key factor in the recycling of cofilin and actin for rapid actin turnover. J. Cell Sci. 115, 1591 – 1601.
14 Tabor, S. and Richardson, C. C. (1992) A bacteriophage T7 RNA polymerase/promoter system for controlled exclusive expression of specific genes. Biotechnology 24, 280 – 284.
15 Rick, M., Ramos Garrido, S. I., Herr, C., Thal, D. R., Noegel, A. A. and Clemen, C. S. (2005) Nuclear localization of Annexin A7 during murine brain development. BMC Neurosci. 6, 25.
16 Libotte, T., Zaim, H., Abraham, S., Padmakumar, V. C., Schneider, M., Lu, W., Munck, M., Hutchison, C., Wehnert, M., Fahrenkrog, B., Sauder, U., Aebi, U., Noegel, A. A. and Karakesisoglou, I. (2005) Lamin A/C dependent localization of Nesprin-2, a giant scaffolder at the nuclear envelope. Mol. Biol. Cell 16, 3411 – 3424.
17 Hasse, A., Rosentreter, A., Spoerl, Z., Stumpf, M., Noegel, A. A. and Clemen, C. S. (2005) Coronin 3 and its role in murine brain morphogenesis. Eur. J. Neurosci. 21, 1155 – 1168.
18. Yuspa, S. H., Hawley-Nelson P., Koehler B. and Stanley J.R. (1980) A survey of transformation markers in differentiating epidermal cell lines in culture. Cancer Res. 40, 4694 – 4703.
19 Claycomb, W. C., Lanson, N. A. B. Jr., Stallworth, S., Egeland, D. B., Delcarpio, J. B., Bahinski, A. and Izzo, N. J. Jr. (1998) HL-1 cells: a cardiac muscle cell line that contracts and retains phenotypic characteristics of the adult cardiomyocyte. Proc. Natl. Acad. Sci. USA 95, 2979 – 2984.
20 Zhang, Z.-G., Bothe, I., Hirche, F., Zweers, M., Gullberg, D., Pfitzer, G., Krieg, T., Eckes, B. and Aumailley, M. (2006) Interactions of primary fibroblasts and keratinocytes with extracellular matrix proteins: contribution of $\alpha_2\beta_1$ integrin. J. Cell Sci. 119, 1886 – 1895.
21 Ainscough, J. F., Rahman, F. A., Sercombe, H., Sedo, A., Gerlach, B., Coverley, D. (2007) C-terminal domains deliver the DNA replication factor Ciz1 to the nuclear matrix. J. Cell Sci. 120, 115 – 124.
22 Krüger, M., Pfitzer, G. and Stehle, R. (2003) Effects of the mutation R145G in human cardiac troponin I on the kinetics of the contraction–relaxation cycle in isolated cardiac myofibrils. J. Chromatogr. B Analyt. Technol. Biomed. Life Sci. 786, 287 – 296.
23 Lehmann-Klose, S., Beinbrech, B., Cuppoletti, J., Gratzl, M., Ruegg, J. C. and Pfitzer, G. (1995) Ca(2+)- and GTP[gamma S]-induced translocation of the glucose transporter, GLUT-4, to the plasma membrane of permeabilized cardiomyocytes

determined using a novel immunoprecipitation method. Pflügers Arch. 430, 333 – 339.
24 Chomczynski, P. and Sacchi, N. (1987) Single-step method of RNA isolation by acid guanidinium thiocyanate-phenol-chloroform extraction. Anal. Biochem. 162, 156 – 159.
25 Spudich, J.A. and Watt, S. (1971) The regulation of rabbit skeletal muscle contraction. I. Biochemical studies of the interaction of the tropomyosin-troponin complex with actin and the proteolytic fragments of myosin. J. Biol. Chem. 246, 4866 – 4871.
26 Eichinger, L., Noegel, A. A. and Schleicher, M. (1991) Domain structure in actin-binding proteins: Expression and functional characterization of truncated severin. J. Cell Biol. 112, 665 – 676.
27 Mika, S. and Rost, B. (2005) NMPdb: Database of Nuclear Matrix Proteins. Nucleic Acids Res. 33, D160 – 163.
28 Yoshida, M. and Horinouchi, S. (1999) Trichostatin and leptomycin. Inhibition of histone deacetylation and signal-dependent nuclear export. Ann. N. Y. Acad. Sci. 886, 23 – 26.
29 Yu, L. G., Fernig, D. G., White, M.R., Spiller, D. G., Appleton, P., Evans, R. C., Grierson, I., Smith, J.A., Davies, H., Gerasimenko, O.V., Petersen, O.H., Milton, J.D. and Rhodes, J.M. (1999) Edible mushroom (*Agaricus bisporus*) lectin, which reversibly inhibits epithelial cell proliferation, blocks nuclear localization sequence-dependent nuclear protein import. J. Biol. Chem. 274, 4890 – 4899.
30 Zhen, Y.-Y., Libotte, T., Munck, M., Noegel, A. A. and Korenbaum, E. (2002) NUANCE, a giant protein connecting nucleus and actin cytoskeleton. J. Cell Sci. 115, 3207 – 3222.
31 Shibata, R., Mori, T., Du, W., Chuma, M., Gotoh, M., Shimazu, M., Ueda, M., Hirohashi, S. and Sakamoto, M. (2006) Overexpression of cyclase-associated protein 2 in multistage hepatocarcinogenesis. Clin. Cancer Res. 12, 5363 – 5368.
32 Yoon, J.-H., Qiu, J., Cai, S., Chen, Y., Cheetham, M. E., Shen, B. and Pfeifer, G. P. (2006) The retinitis pigmentosa-mutated RP2 protein exhibits exonuclease activity and translocates to the nucleus in response to DNA damage. Exp. Cell Res. 312, 1323 – 1334.
33 Bienz, M. and Hamada, F. (2004) Adenomatous polyposis coli proteins and cell adhesion. Curr. Opin. Cell Biol. 16, 528 – 535.
34 Agarkova, I. and Perriard, J.-C. (2005) The M-band: An elastic web that crosslinks thick filaments in the center of the sarcomer. Trends Cell Biol. 15, 477 – 485.
35 Mistry, A. C., Kato, A., Tran, Y. H., Honda, S., Tsukada, T., Takei, Y. and Hirose, S. (2004) FHL5, a novel actin-binding protein, is highly expressed in eel gill pillar cells and responds to wall tension. Am. J. Physiol. Regul. Integr. Comp. Physiol. R1141-R1154.
36 Weins, K., Schwarz, C., Faul, L., Barisoni, W., Linke, A. and Mundel, P. (2001) Differentiation- and stress-dependent nuclear cytoplasmic redistribution of myopodin, a novel actin-bundling protein. J. Cell Biol. 155, 393 – 403.
37 Faul, C., Hüttelmeier, S., Oh, J., Hachet, V., Singer, R. H. and Mundel, P. (2005) Promotion of importin alpha-mediated nuclear import by the phosphorylation-dependent binding of cargo protein to 14 – 3-3. J. Cell Biol. 169, 415 – 424.
38 Bettinger, B. T., Gilbert, D. M. and Amberg, D. C. (2004) Actin up in the nucleus. Nat. Rev. Mol. Cell Biol. 5, 410 – 415.
39 Pederson, T. and Aebi, U. (2005) Nuclear actin extends, with no contraction in sight. Mol. Biol. Cell 16, 5055 – 5060.
40 Grummt, I. (2006) Actin and myosin as transcription factors. Curr. Opin. Genet. Dev. 16, 191 – 196.
41 Schoenenberger, C. A., Buchmeier, S., Sutterlin, R., Aebi, U. and Jockusch, B. M., (2005) Conformation-specific antibodies reveal distinct actin structures in the nucleus and the cytoplasm. J. Struct. Biol. 152, 157 – 168.
42 Jockusch, B. M., Schoenenberger, C. A., Stetefeld, J. and Aebi, U. (2006) Tracking down the different forms of nuclear actin. Trends Cell Biol. 16, 391 – 396.
43 McDonald, D., Carrero, G., Andrin, C., de Vries, G. and Hendzel, M. (2006) Nucleoplasmic β-actin exists in a dynamic equilibrium between low mobility polymeric species and rapidly diffusing populations. J. Cell Biol. 172, 541 – 552.